

Combined loss of p21^{waf1/cip1} and p27^{kip1} enhances tumorigenesis in mice

Rosa A García-Fernández¹, Pilar García-Palencia¹, María Á Sánchez¹, Gabriel Gil-Gómez², Belén Sánchez¹, Eduardo Rollán¹, Juan Martín-Caballero² and Juana M Flores¹

The cell cycle inhibitors p21^{Waf1/Cip1} and p27^{Kip1} are frequently downregulated in many human cancers, and correlate with a worse prognosis. We show here that combined deficiency in p21 and p27 proteins in mice is linked to more aggressive spontaneous tumorigenesis, resulting in a decreased lifespan. The most common tumors developed in p21p27 double-null mice were endocrine, with a higher incidence of pituitary adenomas, pheochromocytomas and thyroid adenomas. The combined absence of p21 and p27 proteins delays the incidence of radiation-induced thymic lymphomas with a higher apoptotic rate, measured by active caspase-3 and cleaved PARP-1 immunoprecipitation. These results provide experimental evidence for a cooperation of both cyclin-dependent kinase inhibitors in tumorigenesis in mice.

Laboratory Investigation (2011) 91, 1634–1642; doi:10.1038/labinvest.2011.133; published online 29 August 2011

KEYWORDS: animal model; cyclin-dependent kinase inhibitor; p27^{Kip1}; p21^{Waf1/Cip1}; tumor development

Mammalian cell proliferation, differentiation and death are regulated by similar molecular mechanisms that are modified by carcinogenesis. Cell cycle progression is monitored by multiple checkpoint mechanisms for ensuring its correct development. The main players of these mechanisms are the cyclin-dependent kinases (CDKs), which bind to regulatory units, named cyclin-forming heterodimeric complexes known as CDK/cyclin complexes. CDKs are also regulated by phosphorylation and negatively regulated by their inhibitors or cyclin-dependent kinase inhibitors (CKIs).¹

p21^{Waf1/Cip1} (hereafter referred to as p21) was the first CKI to be identified and a member of the Cip/Kip family, which also includes p27^{Kip1} and p57^{Kip2} (ref. 2). There are many CKIs, but only p21 has a universal inhibitory activity toward all main CDK complexes.³ In addition, p21 can act as a tumor suppressor and occasionally as an oncogene. As a tumor suppressor, it inhibits CDK2–cyclin E complex, involved in the G1–S phase transition of the cell cycle and CDK1–cyclin A and/or CDK2–cyclin A, required for the passage from S to G2 phase, causing a solid stop cell proliferation.⁴ At the same time, p21 binds to proliferating cell nuclear antigen, blocking its ability to activate replicative DNA polymerase δ and inhibiting DNA replication.⁵

The oncogenic activity of p21 lies in the activation of CDK4/6–cyclin D complexes,⁶ involved in the early G1 phase

by promoting cell cycle progression, and the antiapoptotic capacity of p21.^{7,8} Cytoplasm-localized p21 inhibits the activity of proteins involved in apoptosis, including procaspase-3, caspase-8, caspase-10, stress-activated protein kinases and apoptosis signal-regulating kinase 1.^{9,10}

The first genetic evidence of the involvement of p21 as a tumor suppressor was observed in p21 knockout mouse model that developed spontaneous tumors in aged animals.¹¹ It is known that p21 acts in synergy with other tumor suppressors in different animal models. In p18^{Ink4c}–p21 double-null mice, the presence of p21 accelerates the incidence of pituitary adenomas and lung bronchoalveolar adenomas,¹² and in p53-deficient mice increases the frequency of lymphomas and sarcomas.¹³ In p15^{Ink4a}-null mice, the lack of p21 increases the number of fibrosarcomas and rhabdomyosarcomas¹⁴ and, combined with *Atm* deficiency, enhances the frequency of sarcomas, myeloid leukemias, hepatomas and teratomas.¹⁵

p27^{Kip1} (hereafter referred to as p27), another Cip/Kip family member, has a significant role on cell cycle regulation based on its potent inhibitory activity of CDK2–cyclin E, which results in G1 arrest.¹⁶ Beyond its cell cycle regulation, p27 is also involved in the regulation of other cellular processes such as apoptosis or cell motility, which can be oncogenic under certain circumstances. Thus, cytoplasmic

¹Department of Animal Medicine and Surgery, Veterinary School, Complutense University, Madrid, Spain and ²Barcelona Biomedical Research Park, Barcelona, Spain
Correspondence: Dr JM Flores, MVD, PhD, Department of Animal Medicine and Surgery, Veterinary School, Complutense University, Madrid 28040, Spain.
E-mail: jflores@vet.ucm.es

Received 8 June 2011; revised 19 July 2011; accepted 26 July 2011

p27 modulates actin dynamics by direct regulation of RhoA pathway.¹⁷ Moreover, mislocalization of p27 in the cytoplasm of neoplastic cells is correlated with high degree of malignancy and poor prognosis in some types of human cancer.^{18–22}

p27-deficient mice develop multiorgan hyperplasia and pituitary tumors.^{23–25} This deficiency also seems to have an important role in the spontaneous development of T-cell lymphomas in CD2–cyclin E transgenic mice.²⁶ Moreover, in an p16^{Ink4a}/p19^{Arf}-null mice, p27 deficiency triggers tumor development, induces a higher incidence of lymphomas and significantly increases metastasis. In contrast, p21 deficiency in p16^{Ink4a}/p19^{Arf} mutants does not seem to affect mice survival but changes the tumor range, increasing the incidence of fibrosarcomas.¹⁴ Similarly, mice lacking p27 and CDK4 mutated in R24C position developed a wide spectrum of tumors, including pituitary tumors, with short latency and high penetrance.²⁷

Therefore, there are multiple evidences for the role that either p21 or p27 has in tumorigenesis, alone or in combination with other tumor suppressors and oncogenes.^{14,28–31} In addition, CDK-independent functions have been described for p21 and p27, highlighting their role as oncogenes or in cellular stress in different tissues, implicating p21 and p27 as possible therapeutic targets in some processes.^{32,33}

Up to now, no studies have been described using a double-null murine model for p21 and p27. Thus, the main aim of our work is to study the possible oncogenic cooperation of both CDKIs, analyzing the susceptibility to spontaneous tumorigenesis in a double-null murine model generated in our laboratory.

We have reported previously that in p21-null mice there is a delay in the development of radiation-induced thymic lymphomas due to the potent apoptotic response observed in the thymus, which is independent of p53.^{8,11} On that basis, we wondered whether p21p27 double-null mice could have a decreased susceptibility to radiation-induced carcinogenesis. For this reason, we have also performed a γ -radiation-induced thymic lymphoma in mice deficient in p21 and p27 CKIs.

MATERIALS AND METHODS

Mice

The generation of double-knockout mice for p21 and p27 proteins was initiated by mating p27 knockout male mice with p21 knockout females in a C57BL/6J homogeneous genetic background. The absence of p27 causes female sterility due to an ovulatory defect.²³ Because of this, p21p27 double-KO males were mated to p21 KO p27 +/– females to generate p21p27 double-mutant mice. All the animals were housed in a pathogen-free barrier area at the Barcelona Biomedical Research Park (PRBB).

For γ -radiation-induced tumorigenesis, 1-month-old mice of the different genotypes (p21–/–p27–/–, *n* = 6; p21–/–,

n = 6; p27–/–, *n* = 6; and C57BL/6J wild-type mice, *n* = 6) were irradiated once a week for 4 weeks with a dose of 1.75 Gy from a ¹³⁷Cs source (Schering CIS bio international, IBL 437C H) at a ratio of 2.5 Gy/min.

The husbandry and handling procedures were performed in accordance with current European (Federation of European Laboratory Animal Science Associations) and International (International Council for Laboratory Animal Science) regulations, recommendations and policies for the humane laboratory animal care and use. All animal experiments were performed under the experimental protocol approved by PRBB's Institutional Committee for Care and Use of Animals/IACUC.

PCR Genotyping

Samples of tail were taken from all mice and genomic DNA extracted for genotyping by PCR (Figure 1). Independent PCR reactions were assembled for each allele.

Detection of p21 wild-type allele and p21-null allele used a common sense primer (5'-AAGCCTTGATTCTGATGTGGG C-3'). The antisense primers used were specific for the p21 wild-type allele (5'-TGACGAAGTCAAAGTCCACCG-3') and the p21 knockout allele (5'-GCTATCAGGACATAGCGTT GGC-3').

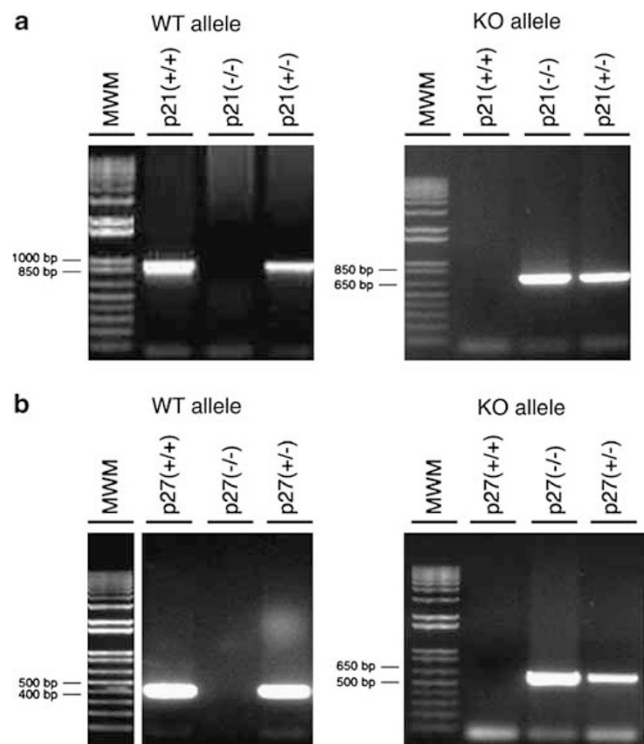


Figure 1 Genotyping of p21 and p27 wild-type (WT) and mutant (KO) alleles by PCR. Representative PCR genotyping results for p21 WT (+/+), heterozygous (+/-) and homozygous (-/-) mice are shown (a). The results of the corresponding tests for p27 WT (+/+), heterozygous (+/-) and homozygous (-/-) mice are shown (b). MWM: DNA molecular weight marker.

In the case of p27, the sense primers used were (5'-TGTC AACGTGAGAGTGTCTAACGG-3') for the wild-type allele and (5'-TGGAACCCTGTGCCATCTCTAT-3') for the p27-null allele. The antisense primers were (5'-AACCCAGCCTGATTGTCTGACGAG-3') for the wild-type and (5'-CCTTCTATCGCCTTCTTGACG-3') for p27-null allele. All the primers for PCR genotyping were used at 0.5 μ M final concentration. PCR buffer (10 \times): 750 mM Tris-HCl (pH 9.0), 500 mM KCl, 200 mM (NH₄)₂SO₄ and 2 mM dNTPs. The MgCl₂ final concentrations used were 3, 1.5, 2.5 and 2 mM for the p21WT, p21 KO, p27WT and p27 KO alleles, respectively. A amount of 0.6 U Biotools DNA polymerase (Biotools B&M Labs, SA, Madrid, Spain) was used per sample. In the case of the p21WT allele, 5% DMSO was included in the PCR reaction.

Thermocycling: step 1, 2 min at 93 °C; step 2, 40 cycles of 30 s at 93 °C, 30 s at 55 °C and an extension of 1 min and 10 s (for p21 KO genotypes) or 1 min (for p27 KO genotypes) at 72 °C; and step 3, 10 min at 72 °C. The DNA bands were separated in a 1% agarose gel (Figure 1), being the sizes of about 900 and 700 bp (for p21WT and KO alleles, respectively) and 500 and 700 bp (for p27WT and KO alleles, respectively).

Necropsy and Pathological Analysis

Mice were monitored daily and killed at any sign of disease. Tissue samples were fixed in 10% buffered formalin, dehydrated in increasing concentrations of ethanol, embedded in paraffin wax, sectioned at 4 μ m and stained with hematoxylin and eosin.

Immunohistochemical staining was performed using the streptavidin–biotin–peroxidase complex method. Tissue sections were processed with 10 mM citrate buffer (pH 6.0) in a microwave (100 °C, 15 min). Endogenous peroxidase activity was inactivated by incubation with 3% hydrogen peroxide in methanol (15 min, room temperature). Tissue sections were incubated in a humidified chamber (overnight, 4 °C) using the following antibodies: rabbit anti ACTH (1/100; Abcam, Cambridge, UK), rabbit anti- β -endorphin (1/50; PROGEN Biotechnik GmbH, Heidelberg, Germany), goat anti-prolactin (1/10; R&D Systems, MN, USA), rabbit anti-chromogranin-A (1/400; Abcam), rabbit anti-Pax5 (1/10; Novus Biologicals, CO, USA), rabbit anti-CD3 (1/300; Abcam), rat anti-F4/80 (clone Cl:A3-1; 1/10; Serotec, Dusseldorf, Germany), rabbit anti-cleaved PARP1 (1/100; Abcam), rabbit anti-active caspase-3 (1/1000; R&D Systems) and rabbit anti-Ki67 (1/800; Novocastra, Newcastle upon Tyne, UK).

The antibodies were diluted in Tris-buffered saline (TBS). For negative controls, primary antibodies were replaced by nonimmune serum. After three rinses in TBS (5 min each), samples were incubated with the secondary antibody. For detecting primary rabbit, goat and rat antibodies, we used biotinylated goat anti-rabbit IgGs, rabbit anti-goat IgGs and rabbit anti-rat IgGs, respectively (1:400; Vector Laboratories,

Burlingame, CA). After 30 min incubation with the secondary antibody, tissue sections were washed in TBS (5 min, 3 times) and immediately incubated for 30 min with streptavidin–peroxidase complex diluted 1:400 in TBS (Zymed Laboratories, Invitrogen, CA, USA). The chromogen was 3-3'-diaminobenzidine (DAB peroxidase substrate kit, Vector Laboratories). Nuclei were counterstained with Harris hematoxylin for 1 min. Images were captured with a DP-10 digital camera in Olympus Vanox microscope at $\times 4$, $\times 10$ and $\times 20$ magnifications.

In γ -radiation-induced thymic lymphomas, the apoptotic index, measured by the percentage of active caspase-3 and cleaved PARP-1-positive cells, and the proliferation index (Ki67-positive cells) were obtained by counting 500 cells per high-power field in five fields of each tumor section.

Statistical Analysis

Survival data were analyzed using Kaplan–Meier survival analysis (SPSS14 and MedCal) and compared using a χ^2 -test. Results were expressed as mean \pm s.e.m. and considered statistically significant when $P < 0.05$.

RESULTS

Study of Spontaneous Tumor Development in p21p27 Double-Null Mice

Animal survival

A 2-year comparative study was performed in a colony of double-null mice for p21 and p27 ($n = 18$) and two more colonies of p21-null mice ($n = 20$) and p27-null mice ($n = 18$). p21p27 double-null mice phenotype was indistinguishable from their wild-type littermates; body and organs weight showed standards values.

The median survival time for p21p27 double-null was 11.6 months, slightly lower than for p27-null animals (12.6 months), and significantly lower than for p21-null mice, the median survival time of which was 15.6 months ($P < 0.001$; Figure 2). In the latter group, three female died quite early (8 months), because of a severe glomerulonephritis, a common disease in p21-deficient female mice.

Spontaneous tumor development in p21p27 double-null mice

The absence of p21 and p27 CKIs lead to the development of tumors with an incidence of 72.2% and an average tumor latency of 11.6 months. In comparison, p21-null mice showed a tumor incidence of 55% with a mean latency of 15.4 months whereas only 50% of the p27-null mice developed tumors with an average tumor latency of 12.6 months (Table 1). Relative tumor incidence is show in Figure 3.

Spontaneous tumor spectrum in p21p27 double-null mice

Histopathological analysis of the spontaneously developed neoplasias in p21p27 double-null mice revealed a broad tumor spectrum (Figure 4). Pituitary tumors were the most frequently observed malignancies, accounting for 33.3%. These neoplasias were composed of polygonal cells arranged

in solid sheets intermingled with fibrovascular stroma. Tumor cells were atypical, with irregular protrusions and pleomorphic nuclei, allowing a diagnosis of pituitary adenomas. They also tended to form hemorrhagic cysts (Figure 4a). The pituitary tumors stained positive for ACTH and β -endorphin, two of the proopiomelanocortin-derived peptides produced in the pars intermedia of the pituitary gland. Tumor cells were negatives for prolactin expression.

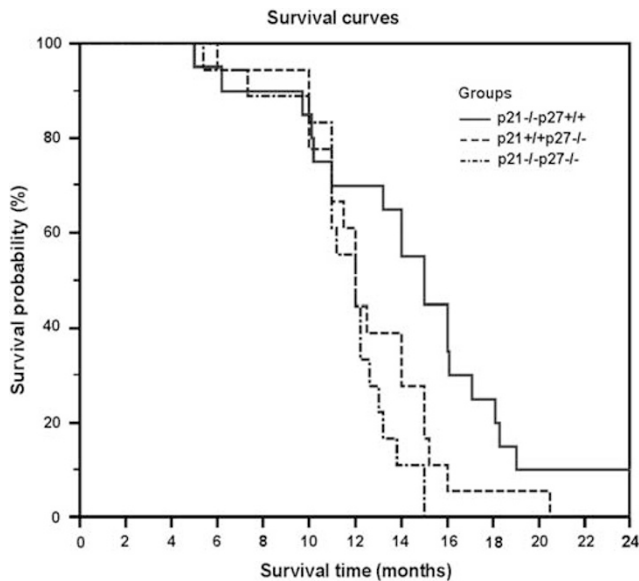


Figure 2 Survival curves of p21- and p27-deficient mice. Mice deficient for p21 (solid line), p27 (dashed line) or both (dash dotted line) were housed in a pathogen-free barrier area and monitored for 24 months. The percentage of mice that were alive was recorded monthly for each group.

Thyroid adenomas appeared only in two double-mutant mice (11.1%), simultaneously with pituitary adenomas. These tumors were composed of colloid-containing follicles lined by a single layer of epithelial cells (Figure 4b).

Benign pheochromocytoma was the second most frequently observed tumor (22.2%); it was mainly composed of chromaffin cells of the adrenal gland medulla (Figure 4c). The tumors found in our study had an expansive growth and were larger than 50% of the normal medulla on histological sections, which is a hallmark in differential diagnosis with medullary hyperplasia in mice.³⁴ Tumor cells were arranged in nests or trabeculae; they were polygonal with large granular cytoplasm and oval central nuclei. Moderate cellular atypia and a low number of mitosis were seen. These tumors showed strong positive immunoreactivity with anti-chromogranin-A antibody (Figure 4d).

p21p27 double-null mice also developed hematopoietic tumors (16.6%). Two of them were histiocytic sarcomas (11.1%) localized in mesenteric lymph nodes, liver and spleen. These tumors were composed of densely packed histiocytic aggregates that infiltrate the tissues and multinucleated giant cells that can be seen occasionally. Histiocytic sarcomas were strongly positive with anti-F4/80 (Figure 4e). Only one mouse developed a B-cell lymphoma (5.5%), composed of uniform round cells with a small basophilic cytoplasm and central round nucleus, which diffusely infiltrated lymph nodes and spleen (Figure 4f).

Finally, other tumors diagnosed were adenoma of the Harderian gland and hepatocellular adenoma (5.5% each) and one mammary adenocarcinoma in a female mouse.

Table 1 Spectrum of spontaneous tumors in the different studied phenotypes

Type of tumor	p21/p27 double-null mice ^a		p21-null mice ^b		p27-null mice ^c	
	Incidence (%)	Latency (months)	Incidence (%)	Latency (months)	Incidence (%)	Latency (months)
Histiocytic sarcoma	11.1 (2/18)	13.5	30 (6/20)	15.9	—	—
Lymphoma	5.5 (1/18)	12.2	5 (1/20)	15.0	—	—
Hemangioma	—	—	10 (2/20)	13.6	—	—
Pituitary adenoma	33.3 (6/18)	10.5	5 (1/20)	15.4	27.7 (5/18)	11.1
Pheochromocytoma	22.2 (4/18)	11.7	—	—	16.6 (3/18)	12.8
Thyroid adenoma	11.1 (2/18)	7.7	—	—	5.5 (1/18)	11.0
Others ^d	16.6 (3/18)	10.4	5 (1/20)	17.3	5.5 (1/18)	14.0

^aOf a total population of 18 animals, 13 developed tumors (72.2%) including 4 that developed up to 3 independent tumors each, yielding a total of 18 tumors.

^bOf a total population of 20 animals, 11 developed tumors (55%).

^cOf a total population of 18 animals, 10 developed tumors (55.5%).

^dA broad spectrum of tumor types was detected at relatively low frequencies. These included a malignant mammary carcinoma (5.5% incidence and 6-month latency), a benign Harderian gland adenoma (5.5% incidence and 11-month latency) and a benign hepatocellular adenoma (5.5% incidence and 15-month latency) in p21/p27 double-null mice; a benign lung adenoma (5% incidence and 19-month latency) in p21-null mice; and a benign duodenal adenoma (5.5% incidence and 14-month latency) in p27-null mice.

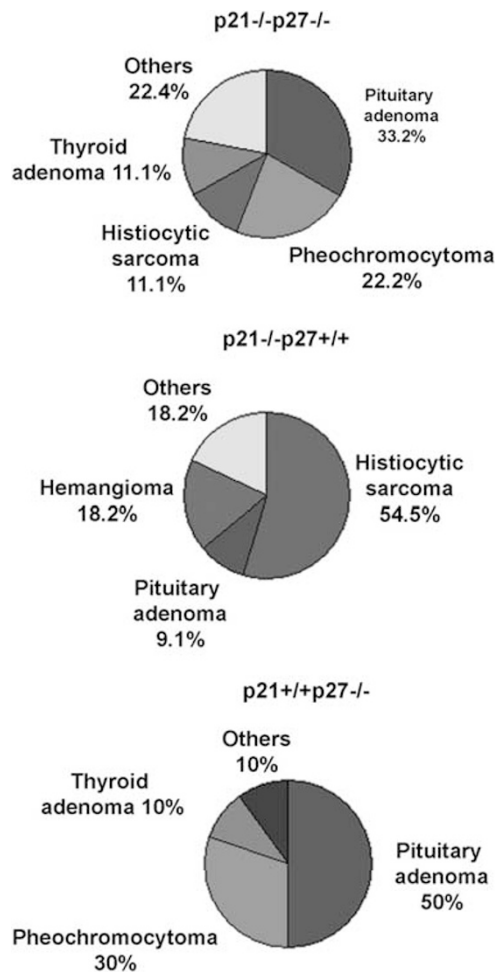


Figure 3 Pie diagrams showing the most common tumor types.

Spontaneous tumor development in p21-null mice

Hematopoietic tumors were the most frequently observed tumor type in p21-null mice, especially histiocytic sarcoma (30%) and B-cell lymphoma (5%).

Hemangiomas were the second most common type of neoplasias (10%). These tumors developed in spleen and liver, and were composed of numerous capillary blood vessels without atypical cells.

p21-null mice also developed some epithelial tumors, such as one pituitary adenoma (5%) and one bronchoalveolar adenoma in the lung (5%).

Spontaneous tumor development in p27-null mice

As it has been reported, pituitary adenoma was the most common type of tumor observed in p27-null mice, with an incidence of 27.7% (Table 1). Interestingly, in our colony we diagnosed pheochromocytomas in three animals, with a latency period of 12.8 months. A single thyroid adenoma was detected (5.5%), with a latency period of 11 months, and a case of intestinal adenoma (5.5%), with a latency period of 14 months.

Study of γ -Radiation-Induced Tumorigenesis in p21p27 Double-Null Mice

To study p21p27 double-null mice susceptibility to radiation-induced carcinogenesis, mice of the different genotypes (p21^{-/-}p27^{-/-}, $n = 6$; p21^{-/-}, $n = 6$; p27^{-/-}, $n = 6$; and C57BL/6J wild-type mice, $n = 6$) were irradiated once a week for 4 weeks with a dose of 1.75 Gy. Animals were daily checked and killed as soon as dyspnea was present. Thymic lymphomas were the only tumor pathology found at necropsy.

The incidence of T-cell lymphomas was lower in p21 KO and p21p27 double-null mice (30% in both groups) than in the rest of the studied groups (100%; Table 2). The development of γ -radiation-induced T-cell lymphoma is responsible for the death of p27^{-/-} mice ($n = 6$) and wild-type mice ($n = 6$) over a period of 8 months after irradiation (Figure 5). In agreement with this, p21-null mice showed a median survival time significantly higher than p27-null mice and wild-type mice ($P < 0.001$, Figure 5). p21p27 double-KO mice showed a significantly higher survival time than p21^{+/+}p27^{-/-} mice ($P < 0.05$) and, although not statistically significant, higher than wild-type animals ($P = 0.05$).

The apoptotic response in γ -irradiated thymic tumors was quantitated by scoring the percentage of cells positive for active caspase-3 and cleaved PARP-1 (Table 2). A higher apoptotic rate was observed in p21p27 double-null and p21^{-/-} mice compared with p27 KO mice and wild-type mice (Figure 6). Proliferation index, measured by Ki67 immunostaining, showed no differences among groups (Figure 6).

DISCUSSION

The object of our study was to investigate the existence of oncogenic cooperation between p21 and p27, both members of the Cip/Kip family of CDKIs, generating for this purpose a colony of mice double null for both proteins. This colony has been followed up and analyzed for 24 months. The results showed that the combined absence of both proteins indicates cooperation between them because double-KO mice suffer of a higher tumor incidence and increased penetrance when compared with p21- or p27-deficient mice.

The phenotype of p21p27 double-mutant mice did not show differences with regard to other mice groups of this study. This is most likely because of the fact that, in contrast to that described in a mixed genetic background,^{23–25} in homogeneous C57BL/6J genetic background no increase in body size is observed in mice lacking p27 protein.

p21p27 double-mutant mice had a median survival time of 11.6 months in a C57BL/6 genetic background. This is significantly lower than the survival of p21-null mice in our study ($P < 0.001$) and their survival in a previous study where p21-null mice were monitored over a period of 16 months.¹¹ Nevertheless, the median survival time in p21p27 double-deficient mice did not show significant differences with regard to p27-null mice (12.6 months). Those facts suggest that the lack of p27 determines the survival time in

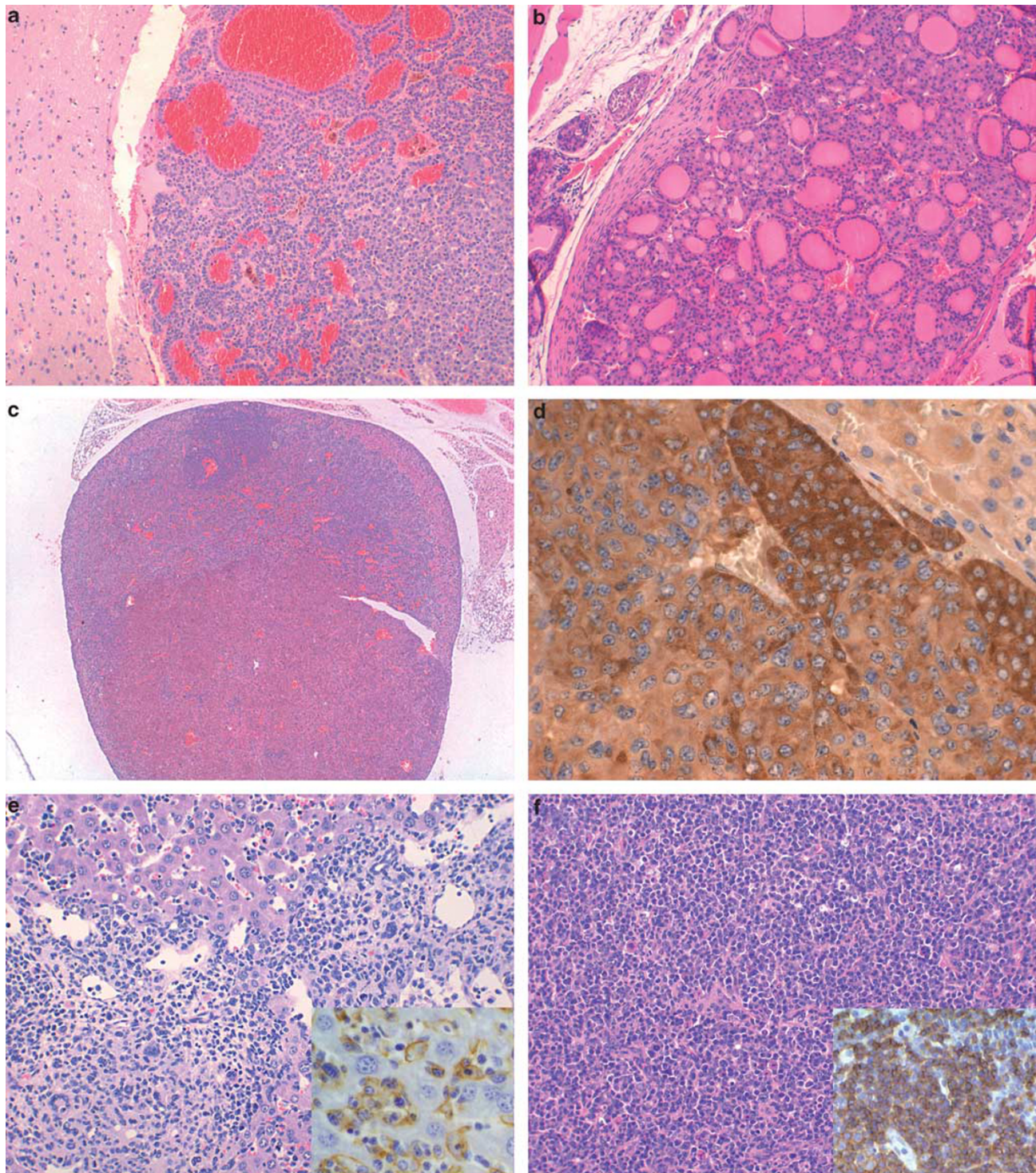


Figure 4 Histological and immunohistochemical analysis of some representative spontaneous tumor developed in p21p27 double-null mice. (a) Pituitary adenoma of pars intermedia (H&E, $\times 100$). (b) Thyroid adenoma (H&E, $\times 100$). (c) Pheochromocytoma, adrenal medullary cells compress cortical area (H&E, $\times 40$). (d) Higher magnification of a pheochromocytoma showing chromogranin-A-positive cells (streptavidin-biotin-peroxidase complex, $\times 400$). (e) Histiocytic sarcoma in the liver (H&E, $\times 200$). The inset shows immunostaining for the macrophage marker F4/80 (streptavidin-biotin-peroxidase complex, $\times 400$). (f) B-cell lymphoma in the lymph nodes (H&E, $\times 200$). In the inset, PAX-5-positive lymphocytes are shown (streptavidin-biotin-peroxidase complex, $\times 200$).

double-null mice. Our results are in agreement with data from the study of the p27 deficiency combined with the lack of p16^{Ink4}-p19^{Arf} in mice, where the median survival time

was only 4.5 months¹⁴ and its combination with the CDK4 KO (6.7 months),²⁷ results that evidenced the negative effect of p27 deletion over the survival time.

Table 2 Evaluation of the apoptotic response (active caspase-3 and cleaved PARP-1) and proliferation index (Ki67) in γ -radiation-induced thymic lymphomas

	Incidence	Active caspase-3 (%)	Cleaved PARP-1 (%)	Ki67 (%)
p21 ^{-/-} p27 ^{-/-}	30% (2/6)	17	36	40
p21 ^{-/-} p27 ^{+/+}	30% (2/6)	19	40	44
p21 ^{+/+} p27 ^{-/-}	100% (6/6)	14	29	43
p21 ^{+/+} p27 ^{+/+}	100% (6/6)	11	22	42

Each tumour from each genotype (p21p27 double-null mice, $n=2$; p27 KO mice, $n=2$; p21 KO mice, $n=4$; and wild-type, mice $n=4$) was analyzed by counting 500 cells in five fields.

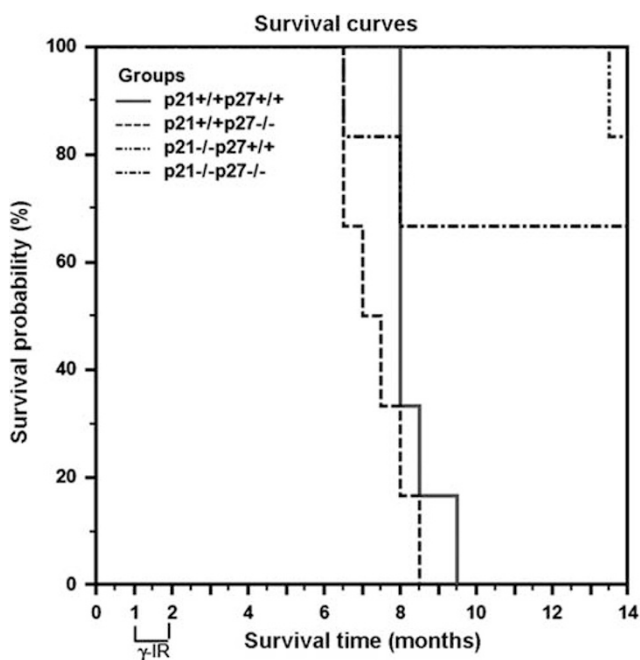


Figure 5 Survival curves of irradiated p21- and p27-deficient mice. One-month-old mice of the indicated genotypes were irradiated with 1.75 Gy once a week for 4 weeks, housed in a pathogen-free barrier area and monitored weekly. Wild-type mice (solid line), p27-null mice (dashed line), p21-null mice (dash dot dotted line) and p21p27 double-null mice (dash dotted line). Percentage of live mice was recorded monthly for each group.

Lethality in p21p27 double-null mice was caused by the development of tumors with a latency period of 11 months. Previous research with p27^{-/-} animals showed lower average tumor latency,²⁷ whereas for p21-null mice the latency period was similar to other published results.¹¹

p21p27 double-null mice develop a broad spectrum of neoplasias. Endocrine tumors (derived from pituitary, adrenal and thyroid glands) were the most common type found, followed by hematopoietic neoplasias, mainly histiocytic sarcomas and lymphomas.

Pituitary adenomas, arising from the pars intermedia, were the most frequently observed tumors (33.3%) and matched those previously observed in p27-null mice.^{23–25,32} The second most common tumor type in p21p27 double-KO mice was pheochromocytoma (22.2%), also highly frequent in our p27-null mice in the C57BL/6 genetic background (16.6%). In fact, pheochromocytomas have also been described in p27^{ck-/-} knock-in mice in 129S4 background.³² In double-mutant Cdk4^{R/R}p27^{-/-}, adrenal medullary hyperplasia and pheochromocytomas have also been described, with significant lower latency period than in the single-mutant Cdk4^{R/R} or p27^{-/-} (ref. 27) mice. However, other studies using p27-null mice in 129SV background only described adrenal medullary hyperplasia,²⁴ or did not make any reference to the development of pretumoral or tumoral lesions in the adrenal gland.^{23,25} This could be related to the different genetic backgrounds used to create the different lines or could be associated with the histological criteria applied to differentiate hyperplasias from neoplasias in the mouse adrenal gland.³⁴ Other epithelial tumor developed in mice double deficient in p21 and p27 proteins was located in thyroid glands. In this type of neoplasias, the impairment of p27 function has been reported as being very frequent.³⁵ Recent studies have demonstrated that the loss of p27 in mice, with targeted overexpression of *TRK-T1* oncogene, enhances thyroid carcinogenesis.³⁶

The most common hematopoietic tumor diagnosed in double-deficient mice was histiocytic sarcoma. This tumor was also the most frequent type observed in p21-null mice in our study as well as in others previously published.¹¹ Interestingly, lymphomas do not develop spontaneously in p27-null mice,^{23–25} but they were detected in p21p27 double-null mice (5.5%).^{26,36}

The broad tumor spectrum observed in p21p27 double-deficient murine model has some resemblances with human neoplasias. Although mutation of *p21* or *p27* genes is rare in human cancer, decreased levels of expression of these proteins correlate with poor prognosis. Thus, reduced p21 levels were observed in colorectal cancer^{37,38} and have been used as a predictor of poor prognosis in human breast cancer^{39,40} and hepatocarcinoma.⁴¹ At this point, it is important to consider that p21 is the major transcriptional target of the tumor suppressor gene *p53*, frequently mutated in human cancer. Additionally, p27 deficiency has been reported in many human tumors of breast, colon and lungs.^{42–44}

p21p27 double-null mice demonstrate the oncogenic cooperation between both CKIs, as p21 deficiency only leads to the development of tumors in aged animals,¹¹ whereas p27-null mice develop only benign pituitary adenomas.^{23–25} The deletion of p21 in this model has a role as a tumorigenesis enhancer similar to that when it is combined with p18^{Ink4c} ^{-/-} mice,¹² *Atm*-null mice¹⁵ or *Trp53* ^{-/-} mice.⁸

The wide variety of tumors that spontaneously develop in double-KO mice suggests that p21 and p27 proteins are

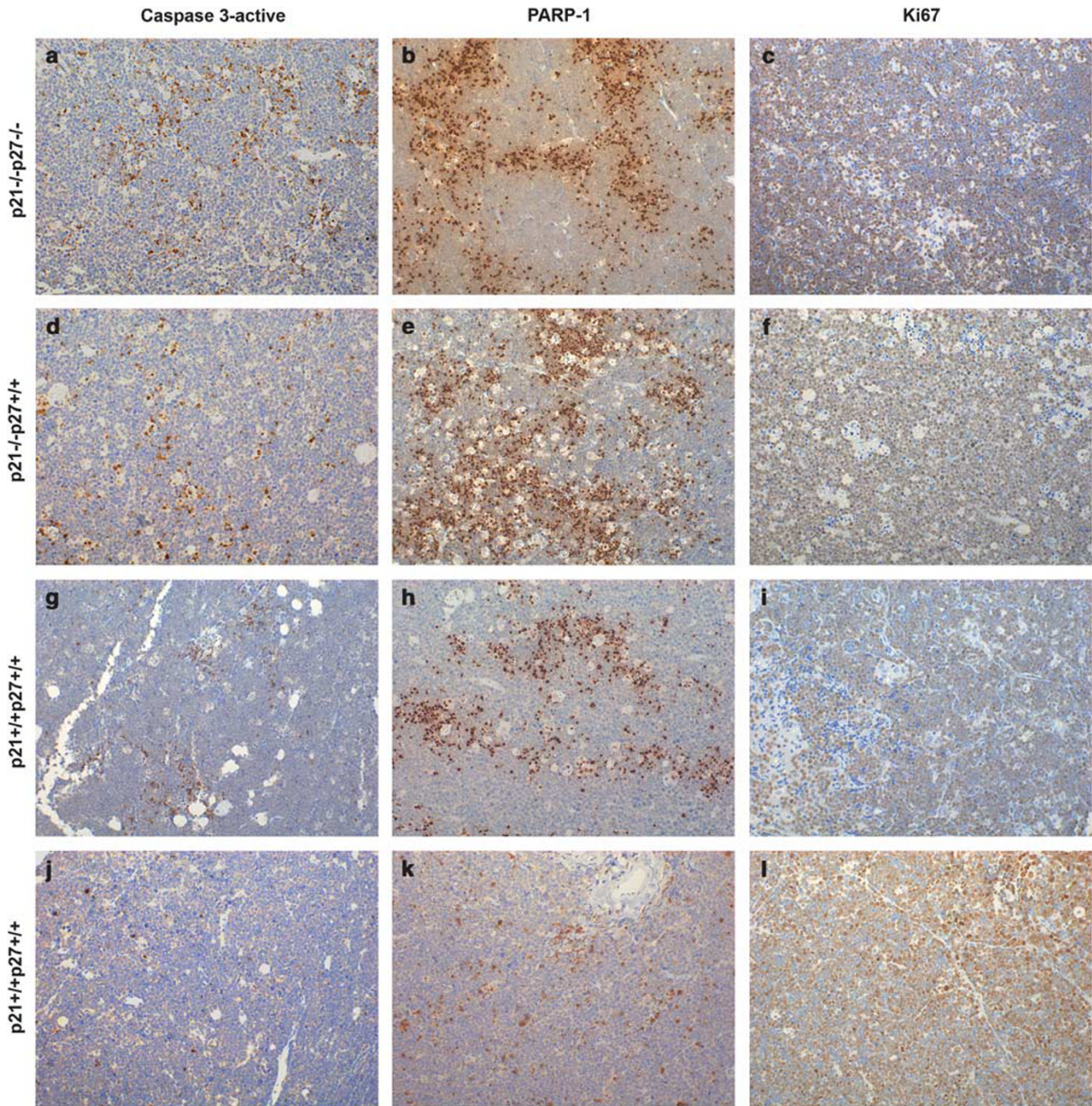


Figure 6 Apoptosis and proliferation index in γ -radiation-induced thymic lymphomas. Immunohistochemical analysis of active caspase-3 (a, d, g, j), cleaved PARP-1 (b, e, h, k) and Ki67 (c, f, i, l) in thymic lymphomas arising in irradiated p21p27 double-null mice, p21-null mice, p27-null mice and wild-type mice, respectively (streptavidin–biotin–peroxidase complex, $\times 100$).

involved in cell cycle regulation, transformation and cancer development in most cell types.^{10,32,45}

p21p27 double-null mice exposed to γ -radiation were more resistant to neoplasias than wild-type or p27-null mice, and showed a higher survival rate post irradiation. This could be explained by the loss of the antiapoptotic effect after p21 ablation, as it has been shown in previous studies performed in p21-null mice, where animals developed an effective apoptotic response in the thymus.¹¹ Our results show the existence of an active apoptotic response in p21p27 double-

null thymic lymphomas using active caspase-3 and cleaved PARP-1 as markers.

To summarize, p21p27 double-null murine model shows high tumor incidence and develops a broad range of neoplasias. This leads to an increase in lethality, demonstrating the cooperative role of p21 and p27 CKIs in tumor suppression.

ACKNOWLEDGEMENTS

This work was granted by Santander Bank and the UCM University (GR 58/08).

DISCLOSURE/CONFLICT OF INTEREST

The authors declare no conflict of interest.

- Sherr CJ, Roberts JM. Cdk inhibitors: positive and negative regulators of G1-phase progression. *Gene Dev* 1999;13:1501–1512.
- el-Deiry WS, Tokino T, Velculescu VE, *et al*. WAF1, a potential mediator of p53 tumor suppression. *Cell* 1993;19:817–825.
- Harper JW, Adami GR, Wei N, *et al*. The p21 Cdk-interacting protein Cip1 is a potent inhibitor of G1 cyclin-dependent kinases. *Cell* 1993;75:805–816.
- Deng C, Zhang P, Harper W, *et al*. Mice lacking p21^{Cip1/waf1} undergo normal development, but are defective in G1 checkpoint control. *Cell* 1995;82:675–684.
- Moldovan GL, Pfander B, Jentsch S. PCNA, the maestro of the replication fork. *Cell* 2007;18:665–679.
- LaBaer J, Garrett MD, Stevenson LF, *et al*. New functional activities for the p21 family of Cdk inhibitors. *Gene Dev* 1997;11:847–862.
- Wang YA, Elson A, Leder P. Loss of p21 increases sensitivity to ionizing radiation and delays the onset of lymphoma in *atm*-deficient mice. *Proc Natl Acad Sci* 1997;94:14590–14595.
- De la Cueva E, García-Cao I, Herranz M, *et al*. Tumorigenic activity of p21^{Waf1/Cip1} in thymic lymphoma. *Oncogene* 2006;25:4128–4132.
- Roninson IB. Oncogenic functions of tumour suppressor p21(Waf1/Cip1/Sdi1): association with cell senescence and tumour-promoting activities of stromal fibroblasts. *Cancer Lett* 2002;179:1–14.
- Abbas T, Dutta A. p21 in cancer: intricate networks and multiple activities. *Nat Rev Cancer* 2009;9:400–414.
- Martin-Caballero J, Flores JM, García-Palencia P, *et al*. Tumor susceptibility of p21^(Waf1/Cip1)-deficient mice. *Cancer Res* 2001;61:6234–6238.
- Franklin DS, Godfrey VL, O'Brien DA, *et al*. Functional collaboration between different cyclin-dependent kinase inhibitors suppresses tumor growth with distinct tissue specificity. *Mol Cell Biol* 2000;20:6147–6158.
- Barboza JA, Liu G, Ju Z, *et al*. p21 delays tumor onset by preservation of chromosomal stability. *Proc Natl Acad Sci USA* 2006;103:19842–19847.
- Martin-Caballero J, Flores JM, García-Palencia P, *et al*. Different cooperating effect of p21 or p27 deficiency in combination with INK4a/ARF deletion in mice. *Oncogene* 2004;28:8231–8237.
- Shen KC, Heng H, Wang Y, *et al*. ATM and p21 cooperate to suppress aneuploidy and subsequent tumor development. *Cancer Res* 2005;65:8747–8753.
- Toyoshima H, Hunter T. p27, a novel inhibitor of G1 cyclin-Cdk protein kinase activity, is related to p21. *Cell* 1994;78:67–74.
- Besson A, Gurian-West M, Schmidt A, *et al*. p27Kip1 modulates cell migration through the regulation of RhoA activation. *Gene Dev* 2004;18:862–876.
- Nakasu S, Nakajima M, Handa J. Anomalous p27kip1 expression in a subset of malignant gliomas. *Brain Tumor Pathol* 1999;16:17–21.
- Sánchez-Beato M, Camacho FI, Martínez-Montero JC, *et al*. Anomalous high p27/KIP1 expression in a subset of aggressive B-cell lymphomas is associated with cyclin D3 overexpression. p27/KIP1-cyclin D3 colocalization in tumor cells. *Blood* 1999;94:765–772.
- Blain WS, Massagué J. Breast cancer banished p27 from nucleus. *Nat Med* 2002;8:1076–1078.
- Rosen DG, Yang G, Cai KQ, *et al*. Subcellular localization of p27kip1 expression predicts poor prognosis in human ovarian cancer. *Clin Cancer Res* 2005;11:632–637.
- Qi CF, Xiang S, Shin MS, *et al*. Expression of the cyclin-dependent kinase inhibitor p27 and its deregulation in mouse B cell lymphomas. *Leuk Res* 2006;30:153–163.
- Fero ML, Rivkin M, Tasch M, *et al*. A syndrome of multiorgan hyperplasia with features of gigantism, tumorigenesis, and female sterility in p27(Kip1)-deficient mice. *Cell* 1996;85:733–744.
- Nakayama K, Ishida N, Shirane M, *et al*. Mice lacking p27(Kip1) display increased body size, multiple organ hyperplasia, retinal dysplasia, and pituitary tumors. *Cell* 1996;31:707–720.
- Kiyokawa H, Kineman RD, Manova-Todorova KO, *et al*. Enhanced growth of mice lacking the cyclin-dependent kinase inhibitor function of p27(Kip1). *Cell* 1996;31:721–732.
- Geisen C, Karsunky H, Yücel R, *et al*. Loss of p27(Kip1) cooperates with cyclin E in T-cell lymphomagenesis. *Oncogene* 2003;22:1724–1729.
- Sotillo R, Renner O, Dubus P, *et al*. Cooperation between Cdk4 and p27kip1 in tumor development: a preclinical model to evaluate cell cycle inhibitors with therapeutic activity. *Cancer Res* 2005;65:3846–3852.
- Martins CP, Berns A. Loss of p27(Kip1) but not p21(Cip1) decreases survival and synergizes with MYC in murine lymphomagenesis. *EMBO J* 2002;21:3739–3748.
- Jackson RJ, Coppola D, Cantor A, *et al*. Loss of the cell cycle inhibitors p21(Cip1) and p27(Kip1) enhances tumorigenesis in knockout mouse models. *Oncogene* 2003;21:8486–8497.
- Damo LA, Snyder PW, Franklin DS. Tumorigenesis in p27/p53- and p18/p53-double-null mice: functional collaboration between the pRb and p53 pathways. *Mol Carcinog* 2005;42:109–120.
- Quereda V, Martinalbo J, Dubus P, *et al*. Genetic cooperation between p21(Cip1) and INK4 inhibitors in cellular senescence and tumor suppression. *Oncogene* 2007;26:7665–7674.
- Besson A, Hwang HC, Cicero S, *et al*. Discovery of an oncogenic activity in p27Kip1 that causes stem cell expansion and a multiple tumor phenotype. *Gene Dev* 2007;15:1731–1746.
- Choudhury AR, Ju Z, Djojotubroto MW, *et al*. Cdkn1a deletion improves stem cell function and lifespan of mice with dysfunctional telomeres without accelerating cancer formation. *Nat Genet* 2007;39:99–105.
- Mohr U. International Classification of Rodent Tumors. The Mouse. Springer. WHO International Agency for Research on Cancer, 2001, pp 4.
- Baldassarre G, Belletti B, Bruni P, *et al*. Overexpressed cyclin D3 contributes to retaining the growth inhibitor p27 in the cytoplasm of thyroid tumor cells. *J Clin Invest* 1999;104:865–874.
- Fedele M, Palmieri D, Chiappetta G, *et al*. Impairment of the p27kip1 function enhances thyroid carcinogenesis in TRK-T1 transgenic mice. *Endocr Relat Cancer* 2009;16:483–490.
- Zirbes TK, Baldus SE, Moenig SP, *et al*. Prognostic impact of p21/waf1/cip1 in colorectal cancer. *Int J Cancer* 2000;89:14–18.
- Mitomi H, Mori A, Kanazawa H, *et al*. Venous invasion and down-regulation of p21(WAF1/CIP1) are associated with metastasis in colorectal carcinomas. *Hepatogastroenterology* 2005;52:1421–1426.
- Winters ZE, Hunt NC, Bradburn MJ, *et al*. Subcellular localisation of cyclin B, Cdc2 and p21(WAF1/CIP1) in breast cancer: association with prognosis. *Eur J Cancer* 2001;37:2405–2412.
- Ping B, He X, Xia W, *et al*. Cytoplasmic expression of p21CIP1/WAF1 is correlated with IKKbeta overexpression in human breast cancers. *Int J Oncol* 2006;29:1103–1110.
- Shiraki K, Wagayama H. Cytoplasmic p21(WAF1/CIP1) expression in human hepatocellular carcinomas. *Liver Int* 2006;26:1018–1019.
- Lloyd RV, Erickson LA, Jin L, *et al*. p27kip1: a multifunctional cyclin-dependent kinase inhibitor with prognostic significance in human cancers. *Am J Pathol* 1999;154:313–323.
- Slingerland J, Pagano M. Regulation of the cdk inhibitor p27 and its deregulation in cancer. *J Cell Physiol* 2000;183:10–17.
- Philipp-Staheli J, Payne SR, Kemp CJ. p27(Kip1): regulation and function of a haploinsufficient tumor suppressor and its misregulation in cancer. *Exp Cell Res* 2001;10:148–168.
- Berton S, Belletti B, Wolf K, *et al*. The tumor suppressor functions of p27(kip1) include control of the mesenchymal/amoeboid transition. *Mol Cell Biol* 2009;29:5031–5045.